Int. J. Electrochem. Sci., 14 **(2019)** 10490 – 10507, doi: 10.20964/2019.11.37

International Journal of
ELECTROCHEMICAL
SCIENCE
www.electrochemsci.org

Corrosion Behavior of Waterborne Epoxy Ester Coatings with Different Composition in NaCl Solution

Zhendong Sun[1,2,3,], Lina Zhao[2], Yong Guan[2], Qiushi Song[1], Qian Xu[1,4], Chuanwei Yan[3]*

[1] School of Metallurgy, Northeastern University, Shenyang 110819, China;
[2] Shenyang Institute of Engineering, Shenyang 110136, China;
[3] Laboratory for Corrosion and Protection of Metals, Institute of Metal Research, Chinese Academy of Sciences, Shenyang 110016, China;
[4] State Key Laboratory of Advanced Special Steel, School of Materials Science and Engineering, Shanghai University, Shanghai 200072, China
[*]E-mail: sunzd@sie.edu.cn

Received: 1 July 2019 / *Accepted:* 26 August 2019 / *Published:* 7 October 2019

In this paper, the effect of water resistance, crosslinking degree, pigments addition, and immersion time on corrosion behavior of the waterborne epoxy ester coatings with different composition in 3.5 wt.% NaCl solution have been studied by electrochemical impedance spectroscopy (EIS). Results show that the coating of higher water resistance and crosslinking degree has higher corrosion resistance. However, much higher crosslinking degree may lead to decreased water resistance of the coating, and it is necessary to minimize the content of hydrophilic groups in the waterborne coating while ensuring a qualified crosslinking degree for improving its corrosion resistance. The waterborne epoxy ester varnish coating without pigments addition degrades quickly in NaCl solution compared with the coating with pigments addition of $ZnMoO_4$ and $Zn_3(PO_4)_2$. For the corrosion evolution of waterborne epoxy ester coating in NaCl solution, it has better shielding effect at 6 h immersion. At 72 h immersion, it still has corrosion protection effect to steel substrate; the NaCl electrolyte has penetrated into the coating but has not reached the coating/substrate interface. At 120 h immersion time, NaCl electrolyte has reached the coating/steel interface, and the steel corrosion has occurred. At 240 h immersion time, serious corrosion attack has occurred on the steel substrate, and the waterborne epoxy ester coating has lost its shielding effect and corrosion protection effect to the underlying steel substrate.

Keywords: Waterborne coating; Epoxy ester coating; Corrosion behavior; NaCl solution; Shielding effect

1. INTRODUCTION

Increasing environmental pressures are forcing the coating industry to minimize the release of volatile organic compounds (VOC) [1]. Many countries in the world have issued regulations to control

the pollution of VOC emission, heavy metals and other pollutants in the paint, and this has boosted the development of environmental-friendly coatings [2-6]. Waterborne coating, as the most important environmental-friendly coating, can reduce the release of VOC [3], and it will absolutely be the main field for development in the future. It has the advantages of energy saving and environmental protection, and has become one of the development directions of coatings industry [4]. However, the application of waterborne coating is still limited due to the relatively poor performance compared with solvent-based coating [5]. Therefore, the research and development related to waterborne coating are bound to attract more and more attention in the future research.

Epoxy resin is a kind of thermoset crystalline polymers, of which molecular structure contains mesogenic unit and epoxy group [6-8]. After being cured, a highly-ordered and deeply-crossed polyer networks structure can be obtained [7]. Therefore, in practice, epoxy resin is gaining more and more applications as binder resin for organic coatings due to its excellent protective properties against corrosion [8]. However, the low adhesion between the epoxy coatings and the underlying metallic substrate and defects in the coating itself has limited the use of epoxy coatings in many areas, such as in marine environments including atmospheric condition and immersion condition. When the interface force between coating and substrate is lower than the surrounding stress, the blister and detachment of the coating will occur, leading to the subsequent corrosion of metallic substrate [9]. Moreover, the incompatibility between coatings and pigments will bring in so many defects that the coatings cannot be compact enough to protect the metallic substrates from the corrosion electrolyte penetration.

The interfacial bonding between waterborne epoxy resin coating and metallic substrates is primarily physical adsorption, which has a low interaction force and this is detrimental for the long term corrosion protection effect of the waterborne coating to the underlying metallic substrate [10]. In this investigation, waterborne epoxy ester resin has been obtained by reaction between ring-opening on epoxy resin and carboxylic acid, and the presence of a large amount of polar bonds such as ether bonds and hydroxyl makes the epoxy ester coating have better adhesion to the steel substrate [11]. Although the lost of epoxy group can lower shielding effect of the coating, the crosslinking between the epoxy ester binder resin and blocked isocyanate can contribute to 3D network structure of the coating and its improved corrosion resistance [12]. To the best of our knowledge, the effects of water resistance, crosslinking degree, pigments addition, and immersion time on the corrosion behavior of waterborne epoxy ester coatings have not been systematically investigated. Therefore, waterborne epoxy ester coatings with different composition have been prepared, and this paper aims to study the effect of water resistance, crosslinking degree, pigments addition, and immersion time on the corrosion behavior of waterborne epoxy ester coatings in 3.5 wt.% NaCl solution. It is believed that this investigation and the findings will be of great theoretical and practical importance for the development of waterborne coating and the understanding of its corrosion behavior in NaCl solution.

2. EXPERIMENTAL

2.1 Materials

Epoxy resin has different types in structures and bisphenol A epoxy resin has been used in this investigation, with its typical structure shown in Eq. (1) [13].

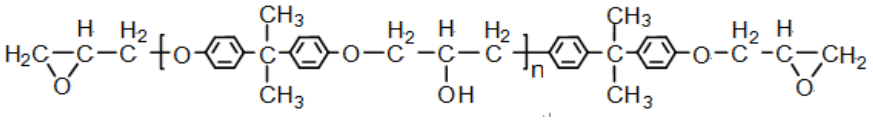

(1)

For the selected waterborne epoxy ester resin, it is obtained by reaction between ring-opening on epoxy and carboxylic acid, and the presence of a large amount of polar bonds such as ether bonds and hydroxyl makes the coating have better adhesion to the underlying steel substrate. Water-dispersible acrylate-modified saturated polyester and epoxy resin were selected as binder resins. Commercialized waterborne blocked isocyanate and waterborne amino resin were selected as crosslinking resins. $ZnMoO_4$ and $Zn_3(PO_4)_2$ were used as pigments.

In this investigation, Q235 low carbon steel sheets of size 100 mm × 100 mm × 2 mm were used for coatings preparation and the steel composition was listed in Table 1.

Table 1. Chemical compositions of the Q235 carbon steel sheets (in wt.%)

Element	C	Si	Mn	S	P	Cu	Fe
Content	0.160	0.210	0.580	0.025	0.017	0.024	Bal.

2.2 Coatings preparation and property characterization

Firstly, selected waterborne epoxy ester resin, pigments and deionized water were proportionally added to a small grinder, and were grinded to slurry with fineness less than 40 μm and good dispersion. Then, crosslinking agent and deionized water were added to the slurry, followed by stirring at high speed for 2 h, filtration, and packaging for use.

The carbon steel sheets were pre-treated by ultrasonic degreasing, rinsing, activation, and drying. The wet coating film on steel surface was obtained by scraper roller, and then baked in oven with temperature of 225 ^{o}C for 40 – 45 s. The obtained waterborne coating samples were kept in a chamber with constant temperature and humidity for test and characterization, and the obtained coating thickness was about 6 – 7 μm. The description of designed waterborne epoxy ester coatings is shown in Table 2. Quanta 2000 scanning electron microscope (SEM) was employed to study the obtained waterborne coating surface morphology.

Salt spray test (3.5 wt.% NaCl solution), immersion test (5.0 wt.% NaCl solution), and methyl ethyl ketone (MEK) scrubbing test were employed to evaluate the corrosion resistance of obtained coating. The water resistance of waterborne coating was evaluated according to standard GB/T 1733-93 “Determination of Resistance to Water of Films”. The salt solution resistance of waterborne coating was evaluated according to standard GB 1763-79 “Determination of Resistance to Chemical Agent of Film”. The crosslinking degree of waterborne coating was determined by solvent extraction method with xylene as solvent. The water absorption of waterborne coating was determined according to standard HGT 3344-2012 “Determination of water absorption of paint film”. The wet adhesion of waterborne coating was determined according to the method in Reference [14].

Table 2. Overall description of the designed coatings used for investigation

Coating	Description
No. 1	Epoxy ester coating of higher wet adhesion and lower water absorption Crosslinking resin: amino resin and blocked isocyanate Pigment: 30 wt.% $ZnMoO_4$ and 15 wt.% $Zn_3(PO_4)_2$
No. 2	Epoxy ester coating of lower wet adhesion and higher water absorption Crosslinking resin: amino resin Pigment: 30 wt.% $ZnMoO_4$ and 15 wt.% $Zn_3(PO_4)_2$
No. 3	Epoxy ester coating of higher crosslinking degree by controlling curing process Crosslinking resin: amino resin Pigment: 30 wt.% $ZnMoO_4$ and 15 wt.% $Zn_3(PO_4)_2$
No. 4	Epoxy ester coating of lower crosslinking degree by controlling curing process Crosslinking resin: amino resin Pigment: 30 wt.% $ZnMoO_4$ and 15 wt.% $Zn_3(PO_4)_2$
No. 5	Epoxy ester varnish coating without pigments addition

2.3 Electrochemical impedance spectroscopy (EIS)

EIS measurements of the waterborne epoxy ester coatings carried out employing the classic three-electrode system by EG&G PARSTAT2273 electrochemical workstation. A platinum plate with 4 cm^2 area and saturated calomel electrode (SCE) were selected as the counter electrode and the reference electrode, respectively. Waterborne coating with test area of 10 cm^2 was used as working electrode. The frequency range for EIS measurement was from 100 kHz to 10 mHz with a 5 mV amplitude signal at open circuit potential, and the measured EIS data were fitted using the commercial software "Zsimpwin". Before measurement, each sample was immersed in the test electrolyte for 1200 s to reach a steady state, and all the EIS were carried out in 3.5 wt.% NaCl solution at 25 ± 1 ^oC.

3. RESULTS AND DISCUSSION

3.1 Brief overview on protection mechanism of organic coating

As one of the most widely used protection measures, organic coatings has always been increasing gained attention worldwide and the corrosion protection mechanism mainly lies in its shielding effect and electrochemical protection effect to the underlying metallic substrates [15].

As to the shielding effect, organic coating itself can prevent the contact of corrosion electrolyte to the underlying metallic substrate, and this effect requires the coating possessing properties of lower water permeability, lower oxygen permeability, lower ions permeability, and good ability in moisture resistance and adhesion [16]. Although no organic coating can effectively inhibit the penetration of water and oxygen to the metallic substrates, the shielding effect provided by the coating is mainly due to its lower ions permeability and good adhesion ability to moisture attack [17]. In fact, the coating

adhesion to underlying substrate in wet condition has no close relation with that in dry condition, but has close relation with its capacity in water absorption [8]. The water arrived at the coating/substrate interface can destroy the interactions between coating and substrate, leading to destruction in the adhesion [18]. Studies have shown that the decisive factor for organic coating corrosion is not the permeability of the coating, but the adhesion to substrate in presence of corrosion electrolyte [17-20]. As to the sequence of corrosion occurrence on substrate surface and adhesion disappearance of organic coating, EIS study by Westing [21] shows that the substrate corrosion occurs after the coating adhesion disappearance. Therefore, when the wet adhesion disappears, the coating loses its shielding effect [22], and subsequently the underlying substrate corrosion occurs.

As to the electrochemical protection mechanism, the pigments in the organic coating can affect the corrosion process so as to achieve protection effect of the coating and underlying substrate [23]. Usually, the pigments can have both the shielding effect and the electrochemical protection effect [24]. Pigments of lamellar structure can complicate the diffusion penetration path of corrosion electrolyte and can lower the permeability of organic coating [25]. In practice, most of the used pigments have certain solubility in water and their penetration to coating/substrate interface can offer electrochemical protection to the substrate for a long time [26]. In addition, the formed pigment corrosion compounds with higher volume can block or fill up the pores in organic coating, inhibiting further corrosion attack of electrolyte to substrate [25]. On the other hand, galvanic effect by pigments or their corrosion compounds can attract more corrosion ions accumulation at the substrate surface and can increase the electrolyte osmotic pressure [27-28], both of which increases the detachment tendency of the organic coating to the underlying substrate. In addition to the cathodic protection effect by pigments, some pigments of anti-rusting chemicals usually have corrosion inhibition effect and passivation effect [29].

3.2 Effect of water resistance on corrosion behavior of waterborne coating

As discussed above, water penetration in the coating is not the deciding factor for underlying substrate corrosion, but the wet adhesion determines the protection effect of organic coating [30]. In fact, the wet adhesion of waterborne organic coating is closely related to its water resistance. Therefore, Coating No. 1 and Coating No. 2 of different water resistance have been prepared to study the effect of water resistance on the waterborne coating corrosion behavior in 3.5 wt.% NaCl solution. The general coating properties of the two coatings are listed in Table 3.

Table 3. Characteristic of the designed environmental-friendly coatings of different water resistance

Coating	Wet adhesion (h)	Water absorption (%)	Crosslinking degree (%)	Anti-MEK wiping test (time)	Immersion test (h)*
No. 1	102	7	81	120 – 130	140
No. 2	84	15	80	120 – 130	100

* Corrosion and/or blistering occurs after immersion in 5.0 wt.% NaCl solution

Figure 1 shows the Nyquist diagrams for Coating No. 1 and Coating No. 2 in 3.5 wt.% NaCl solution at immersion time of 6 h and 96 h. Fig. 1(a) and Fig. 1(a') show that both Coating No. 1 and Coating No. 2 have similar Nyquist diagram features with a single capacitive loop at 6 h immersion time, indicating their similar corrosion protection effects to the underlying steel sheet at this time. However, as the immersion time proceeds to 96 h, the Nyquist diagrams in Fig. 1(b) and Fig. 1(b') have obviously different features, indicating the different corrosion protection effects of the two coatings to steel substrate at this time. For Coating No. 1, Nyquist diagrams in Fig. 1(a) and Fig. 1(b) show that only one time constant has been observed during the whole immersion time of 96 h, indicating no corrosion occurring on the underlying steel substrate during the whole immersion time of 96 h. Nevertheless, for Coating No. 2, a new time constant has been observed at lower frequency range in Fig. 1(b'), indicating the corrosion occurring on the underlying steel substrate at 96 h immersion time [31]. Therefore, Nyquist diagrams evolution of the two coatings has also indicated that the water resistance has obvious effect in corrosion behavior and resistance of the waterborne coating in 3.5 wt.% NaCl solution.

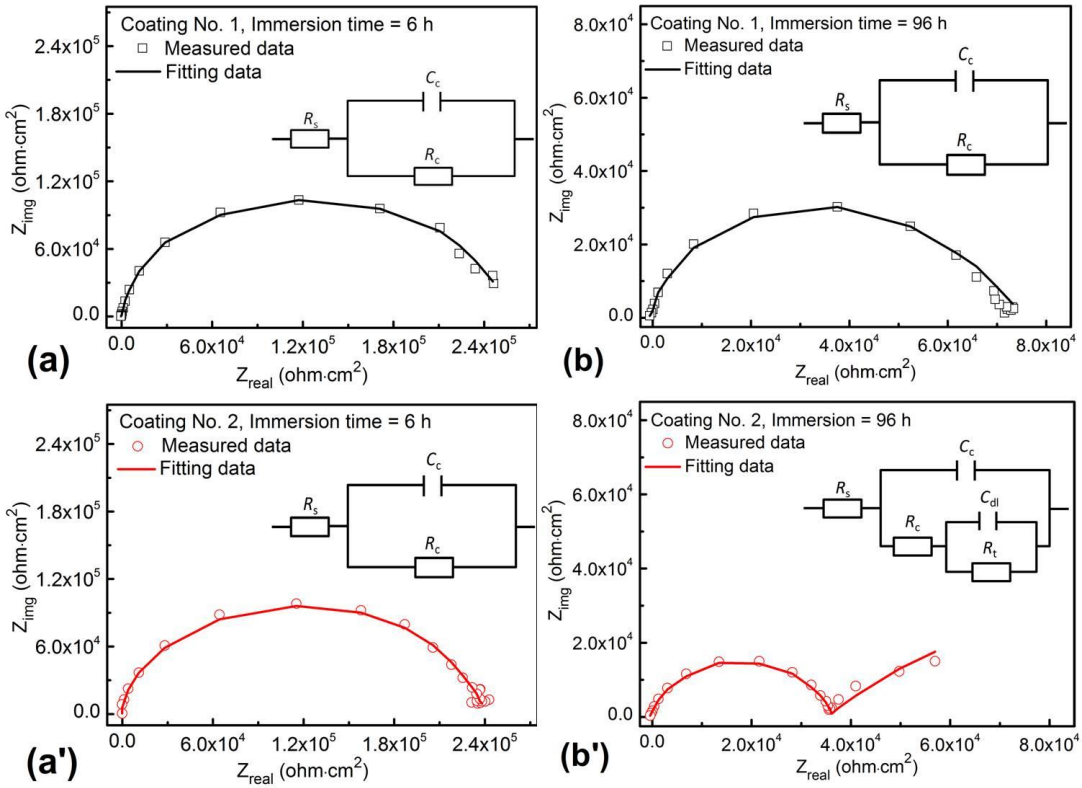

Figure 1. Nyquist diagrams for Coating No. 1 (a) and (b), and Coating No. 2 (a') and (b') in 3.5 wt.% NaCl solution as a function of immersion time

Equivalent circuits have been used to fit the EIS data to further understand the effect of water resistance on the waterborne coating corrosion behavior in 3.5 wt.% NaCl solution. Usually, organic coating is usually considered as an insulating layer, and it can achieve the protection purpose to underlying substrate by preventing or retarding the penetration of corrosion electrolyte to coating/substrate interface [32]. Although water can always penetrate into the coating via the swelling

of coating itself and the micro-pores left on the coating surface due to solvents volatilization, the coating can also act as an insulation layer to isolate the connection between water and substrate metal, as long as the water does not reach the coating/substrate interface [33]. For Nyquist diagrams in Fig. 1(a), Fig. 1(b) and Fig. 1(a'), only one single capacitive loop has been observed during the whole frequency ranges, indicating that only one time constant exists and NaCl solution has not penetrated to the coating/substrate interface [34]. Under this condition, the equivalent circuit for EIS data fitting given at the upper-right corner of Fig. 1(a), Fig. 1(b) and Fig. 1(a') can be expressed by Eq. (2):

$$Z = R_{\mathrm{s}} + \frac{1}{\frac{1}{R_{\mathrm{c}}} + \mathrm{j}\omega C_{\mathrm{c}}} \tag{2}$$

where R_s is solution resistance; C_c is coating capacitance, and R_c is coating resistance.

When the penetration of NaCl solution into the coating reaches a saturation state, the capacitance C_c will not show an obvious increasing trend as the immersion time further proceeds [35], due to the less obvious change in dielectric constant of the coating caused by electrolyte penetration. However, as NaCl solution penetrates through the coating and arrives at coating/substrate interface, as well the formation of corrosion cells at the interface, the measured EIS spectra will exhibit features of two time constants as shown in Fig. 1(b') [36]. At this time, NaCl solution at the interface can both cause the steel corrosion and destroy the coating adhesion to steel substrate, leading to the detachment and blisters formation on coating surface; nevertheless, there is still no presence of obvious visible macro-pores on the coating surface at this time. Under this condition, the corresponding equivalent circuit for EIS data fitting given at the upper-right corner of Fig. 1(b') can be expressed by Eq. (3):

$$Z = R_{\mathrm{s}} + \frac{1}{\mathrm{j}\omega C_{\mathrm{c}} + \frac{1}{R_{\mathrm{c}} + \frac{1}{\mathrm{j}\omega C_{\mathrm{dl}} + \frac{1}{R_{\mathrm{t}}}}}} \tag{3}$$

where R_s is solution resistance; C_c is coating capacitance; R_c is coating resistance; C_{dl} is double layer capacitance, and R_t is substrate dissolution resistance.

Usually, the variation of C_c and R_c can reflect the changes in penetration of NaCl solution into the waterborne coating [37]. The fitted C_c and R_c of the two coatings at immersion time of 6 h and 96 h are shown in Figure 2. The standard deviations x^2 were in the order of 10^{-5}, and the relative error for each parameter was less than 10 %. Clearly, with the penetration of NaCl solution into the two coatings, C_c increases and R_c decreases as the immersion time proceeds during the 96 h immersion time. Fig. 2(a) shows that Coating No. 1 has a higher R_c than Coating No. 2 at 6 h immersion, but the difference is small, indicating the ideal shielding effect of the two coatings to the underlying steel substrate at this time. At 96 h immersion time, although R_c of the two coatings decreases obviously, the decreasing rate of Coating No. 2 is greater than that of Coating No. 1, indicating a much more serious corrosion damage for Coating No. 2 during the immersion period from 6 h to 96 h. For C_c evolution in Fig. 2(b), it has an inverse proportion relationship with R_c evolution in Fig. 2(a). In addition, C_c for Coating No. 1 increases a little, but it increases greatly for Coating No. 2, also indicating much more

serious corrosion damage for Coating No. 2 during the immersion period from 6 h to 96 h. Moreover, the obviously increased C_c for Coating No. 2 also indicates that NaCl solution has penetrated through the coating and arrives at the coating/steel interface, and the non-obvious change in C_c for Coating No. 1 indicates that NaCl solution has not penetrated through the coating.

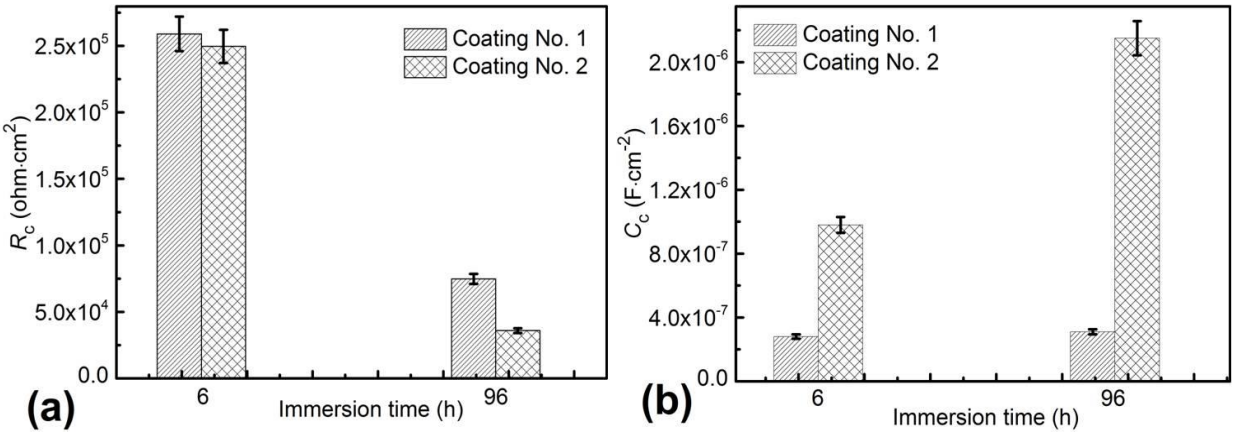

Figure 2. Fitted R_c (a) and C_c (b) evolution of Coating No. 1 and Coating No. 2 at immersion time of 6 h and 96 h

Based on Nyquist diagrams analysis and equivalent circuit fitting of EIS data for Coating No. 1 and Coating No. 2, it can be concluded that Coating No. 1 has a better corrosion resistance than Coating No. 2. This is in accordance with the immersion test result in Table 3. Besides, Table 3 also shows that the two waterborne coatings have almost the same crosslinking degree and MEK wiping test resistance, indicating almost the same molecular free-volume holes in the two coatings, i.e. the same penetration paths for water in the two coatings. Meanwhile, the as-obtained surface morphology observation in Figure 3 shows that both of the two coatings have a compact surface without defects of pin-like holes and cracks. This indicates that the water resistance of the two coatings is responsible for their difference in corrosion behavior and resistance during the whole immersion time. Therefore, waterborne organic coating of higher water resistance can contribute to its better corrosion resistance.

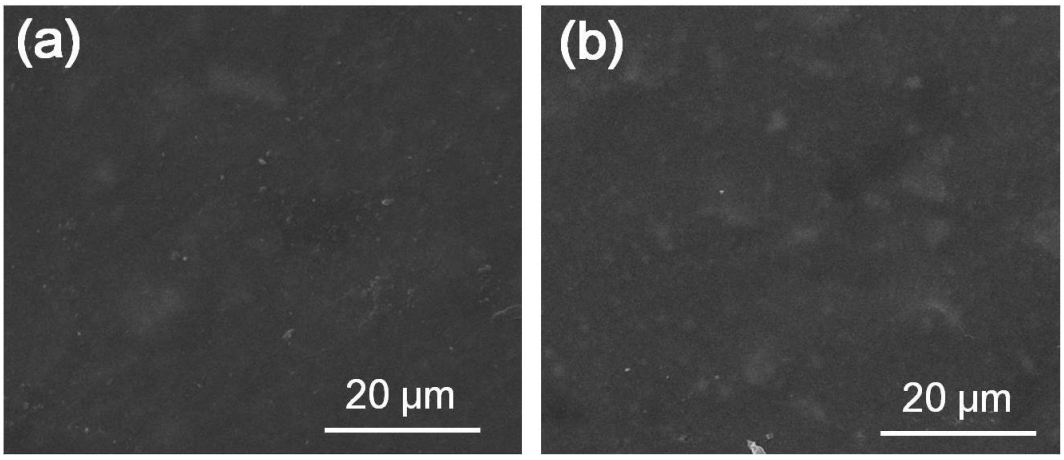

Figure 3. SEM observations of the as-obtained two waterborne coatings. (a) Coating No. 1; (b) Coating No. 2

Although Coating No. 1 has almost the same free-volume holes and surface porosity with Coating No. 2, the presence of a large number of hydrophilic ester bonds, carboxyl groups and ether bonds in Coating No. 2 may be responsible for its lower corrosion resistance. These hydrophilic bonds can unite with water to enhance the penetration of NaCl solution, leading to increased average pore size in the swollen coating [38]. When the coating loses its adhesion to underlying substrate, the corrosion of steel occurs. Although there also are ester bonds, carboxyl groups and ether bonds in Coating No. 1, the formation of urethane bonds by blocked isocyanate crosslinking resin makes the coating have better hydrolysis resistance [9]. Moreover, the waterborne isocyanate itself can act as inner crosslinking agent and can provide many crosslinking points for the coating curing at baking condition. Besides, mutual crosslinking and penetration of amino resin and isocyanate can lower the activity of hydrophilic groups in the binder resin of Coating No. 1 [39-40]. The wet adhesion of Coating No. 1 is 102 h and the water absorption is 7 % as shown in Table 3, and no corrosion has been observed on the underlying steel after immersion for 96 h. This fact indicates that the corrosion of underlying steel occurs after the adhesion lost of the waterborne coating. Therefore, the wet adhesion of waterborne coating is critical for its shielding effect and protection effect to the underlying steel substrate, and it is an important index in evaluating the corrosion resistance of waterborne coating. For the preparation of waterborne coating, it is very necessary to lower the amount of hydrophilic groups to improve water resistance of the coating.

3.3 Effect of crosslinking degree on corrosion behavior of waterborne coating

To investigate the effect of crosslinking degree on corrosion behavior of waterborne organic coating in 3.5 wt.% NaCl solution, Coating No. 3 and Coating No. 4 of different crosslinking degrees have been prepared by controlling the curing conditions, and the general coating properties are listed in Table 4. Clearly, Coating No. 3 has almost the same water absorption level with Coating No. 4, indicating the similar level in hydrophilic group content in the two waterborne coatings. However, Coating No. 3 of higher crosslinking degree has salt spray test resistance up to 430 h, and it is 400 h for Coating No. 4 of lower crosslinking degree, indicating the better corrosion resistance brought by higher crosslinking degree of Coating No. 3 than Coating No. 4 in 3.5 wt.% NaCl solution. As discussed above, the shielding effect and hydrophobic effect of organic coating to water and other corrosion electrolytes is critical to corrosion resistance of the coating. Although no organic coating can effectively inhibit the penetration of water and O_2, the variations in coating porosity (intermolecular free-volume holes and physical ones) always make the coating have great difference in its corrosion resistance and penetration resistance to corrosion electrolyte [41]. Moreover, the large difference in crosslinking degree between Coating No. 3 and Coating No. 4 indicates the difference in space between molecules of the two coatings. Coating No. 3 has lower free-volume holes, and thus the possibility of water and electrolytes penetration is lower and the penetration path for electrolytes is longer and complicated [42]. Therefore, Coating No. 3 of higher crosslinking degree has better shielding effect and corrosion resistance than Coating No. 4 in 3.5 wt.% NaCl solution, as also indicated by the salt spray test in Table 4.

Table 4. Characteristic of the designed environmental-friendly coatings of different crosslinking degree

Coating	Wet adhesion (h)	Water absorption (%)	Crosslinking degree (%)	Salt spray test (h)*
No. 3	104	7	83	430
No. 4	88	8	63	400

* Corrosion and/or blister area width < 2 mm

Figure 4 shows Nyquist diagrams for Coating No. 3 and Coating No. 4 in 3.5 wt.% NaCl solution at immersion time of 6 h and 96 h. Fig. 4(a) and Fig. 4(a') show that Coating No. 3 and Coating No. 4 have similar Nyquist diagram features with a single capacitive loop at 6 h immersion time, indicating their similar corrosion behavior at this time. However, as the immersion time proceeds to 96 h, Nyquist diagrams in Fig. 4(b) and Fig. 4(b') have obviously different features, indicating the different corrosion behavior at this time. For Coating No. 3, Nyquist diagrams in Fig. 4(a) and Fig. 4(b) show that only one time constant has been observed during the whole immersion time of 96 h, indicating no corrosion occurring on the underlying steel substrate during the whole immersion time of 96 h. Nevertheless, for Coating No. 4, a new time constant has been observed at lower frequency range in Fig. 4(b'), indicating the corrosion occurrence on the steel substrate at 96 h immersion time [37].

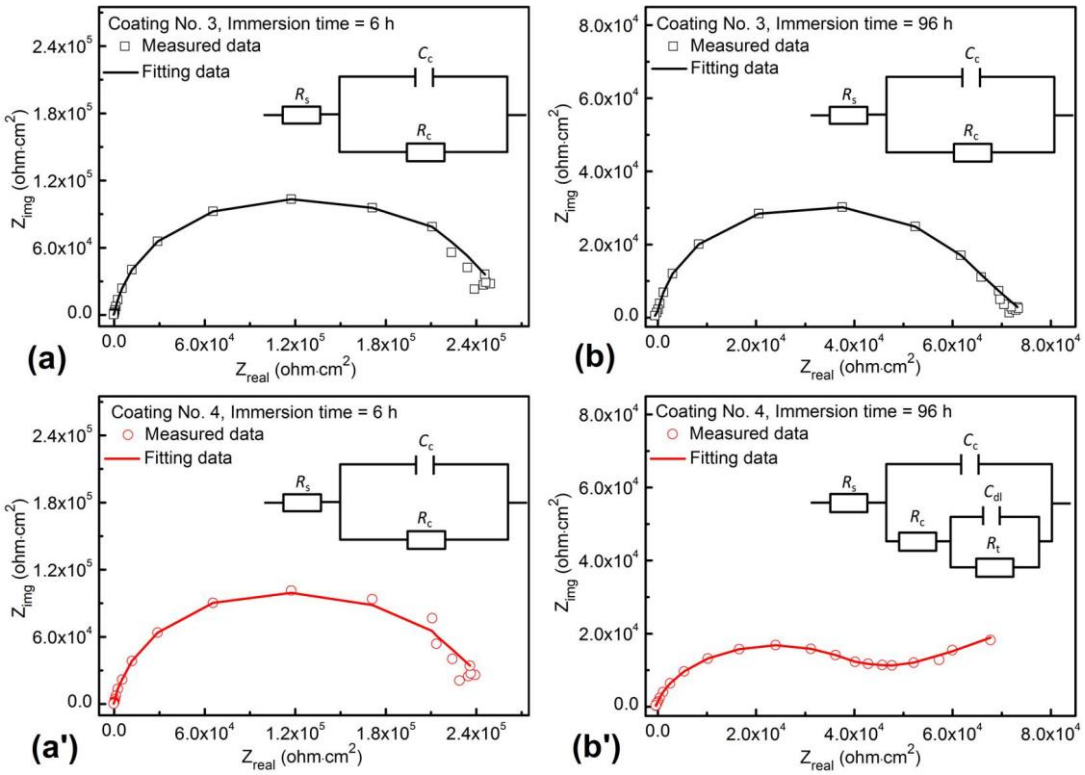

Figure 4. Nyquist diagrams for Coating No. 3 (a) and (b), and Coating No. 4 (a') and (b') in 3.5 wt.% NaCl solution as a function of immersion time

Equivalent circuits have also been used to fit the EIS data to further understand the effect of crosslinking degree on the waterborne coating corrosion behavior in 3.5 wt.% NaCl solution. For Nyquist diagrams in Fig. 4(a), Fig. 4(b) and Fig. 4(a'), only one single capacitive loop has been observed during the whole frequency ranges, indicating that only one time constant exists and NaCl solution has not penetrated to the coating/substrate interface [37]. Under this condition, the corresponding equivalent circuit for EIS data fitting given at the upper-right corner of Fig. 4(a), Fig. 4(b) and Fig. 4(a') can also be expressed by Eq. (1). For Nyquist diagram in Fig. 4(b'), the corresponding equivalent circuit for EIS fitting data given at the upper-right corner of Fig. 4(b') can be expressed by Eq. (2). The fitted C_c and R_c of Coating No. 3 and Coating No. 4 after 6 h and 96 h immersion are shown in Figure 5. The standard deviations x^2 were in the order of 10^{-5}, and the relative error for each parameter was less than 10 %. Clearly, C_c increases and R_c decrease of both Coating No. 3 and Coating No. 4 as the immersion time proceeds during the 96 h immersion time. Fig. 5(a) shows that Coating No. 3 of higher crosslinking degree has a higher R_c than Coating No. 4 at 6 h immersion, indicating the better corrosion resistance of Coating No. 3 than Coating No. 4, and this is in accordance with the salt spray test in Table 4. Besides, both Coating No. 3 and Coating No. 4 have a much higher R_c at 6 h immersion, indicating the ideal shielding effect of the two waterborne coatings to the underlying steel substrate at this time. At 96 h immersion, although R_c of the two coatings decreases obviously, the decreasing rate of Coating No. 4 is higher than that of Coating No. 3, indicating a much more serious corrosion damage for Coating No. 4 during the immersion period from 6 h to 96 h. For C_c evolution in Fig. 5(b), it has an inverse proportion relationship with R_c in Fig. 5(a). In addition, C_c for Coating No. 3 increases a little, but it increases greatly for Coating No. 4, also indicating the more serious corrosion damage for Coating No. 4 during the immersion period from 6 h to 96 h. Moreover, the obviously increased C_c for Coating No. 4 also indicates that NaCl solution has penetrated through the coating and arrives at the coating/steel interface, and the non-obvious change in C_c for Coating No. 3 indicates that NaCl solution has not penetrated through the coating. Therefore, EIS measurements show that waterborne organic coating of higher crosslinking degree can contribute to its better corrosion resistance in 3.5 wt.% NaCl solution.

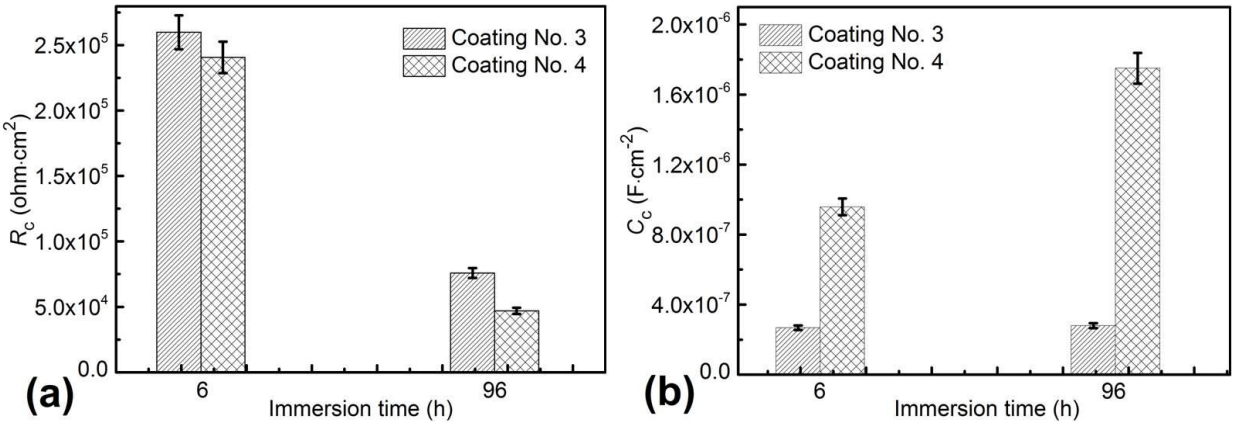

Figure 5. Fitted R_c (a) and C_c (b) evolution of Coating No. 3 and Coating No. 4 at immersion time of 6 h and 96 h

To sum up, water resistance and crosslinking degree are factors closely related to the shielding effect and corrosion protection effect of waterborne organic coating, and there is synergetic effect with each other of the two factors. Increasing crosslinking degree of the waterborne coating can improve its water resistance, and poor water resistance can also destroy the crosslinking groups in the coating. Meanwhile, it should bear in mind that the corrosion process of waterborne coatings is more complex. More weak polar groups by crosslinking resin can contribute to enhanced crosslinking degree of the coating, however, the water resistance decreases obviously. This is why the coating crosslinked by amino resin usually has poor corrosion resistance as evidenced by Coating No. 2 in Table 3. Therefore, for improving the coating corrosion resistance, it is necessary to minimize the content of hydrophilic groups in the waterborne organic coating while ensuring a qualified crosslinking degree of the coating. In this study, we found that for crosslinking resin selection, blocked isocyanate behaves better than amino resin in improving the corrosion resistance of the waterborne epoxy ester coating.

3.4 Effect of pigments addition on corrosion behavior of waterborne coating

Environmental-friendly waterborne organic coating requires low carcinogenic and teratogenic heavy metals pollution [43], and thus in this investigation, $ZnMoO_4$ and $Zn_3(PO_4)_2$ with low toxicity were selected as pigments. Epoxy ester varnish Coating No. 5 has been prepared and Coating No. 1 with pigments addition of 30 wt.% $ZnMoO_4$ and 15 wt.% $Zn_3(PO_4)_2$ has been used for comparison. Figure 6 shows Nyquist diagrams for Coating No. 1 and Coating No. 5 in 3.5 wt.% NaCl solution at immersion time of 6 h and 120 h. Fig. 6(a) and Fig. 6(a') show that Coating No. 1 and Coating No. 5 have similar Nyquist diagram features with a single capacitive loop at 6 h immersion time, but Coating No. 5 has a much lower capacitive loop diameter than Coating No. 1, indicating the great corrosion protection effect of pigments addition to the waterborne coating. As the immersion time proceeds to 120 h, Nyquist diagrams in Fig. 6(b) and Fig. 6(b') have obviously different features, indicating the totally different corrosion behavior at this time. For Coating No. 1, Nyquist diagram in Fig. 6(b) shows that two time constants have been observed after immersion time of 120 h. Nevertheless, for Coating No. 5, Nyquist diagram in Fig. 6(b') shows that one totally different time constant has been observed at lower frequency range in Fig. 6(b'), indicating the totally different corrosion behavior of the coating at 120 h immersion compared with that at 6 h immersion [44]. At this time, the waterborne coating has lost its corrosion protection effect to the underlying steel substrate, indicating that the varnish epoxy ester coating without pigments addition has poor corrosion resistance. As to the anti-corrosion mechanism, MoO_4^{2-} in $ZnMoO_4$ can adsorb on galvanized steel surface with the formation of a passive film and make the steel passivated [45-47]. PO_4^{3-} in $Zn_3(PO_4)_2$ can form complex protective film and make the steel substrate oxidized. However, in the formulation design of waterborne coatings, the ratio of pigments to binder resins should be carefully considered. Lower content of pigments can be consecutively dispersed in the binder resin matrix, but much higher pigments content may lead to the fact that matrix binder resin cannot completely fill the voids between pigments [47]. In this condition, the increased un-filled gaps can facilitate the electrolyte penetration and lower the shielding effect and corrosion protection effect of the waterborne coating.

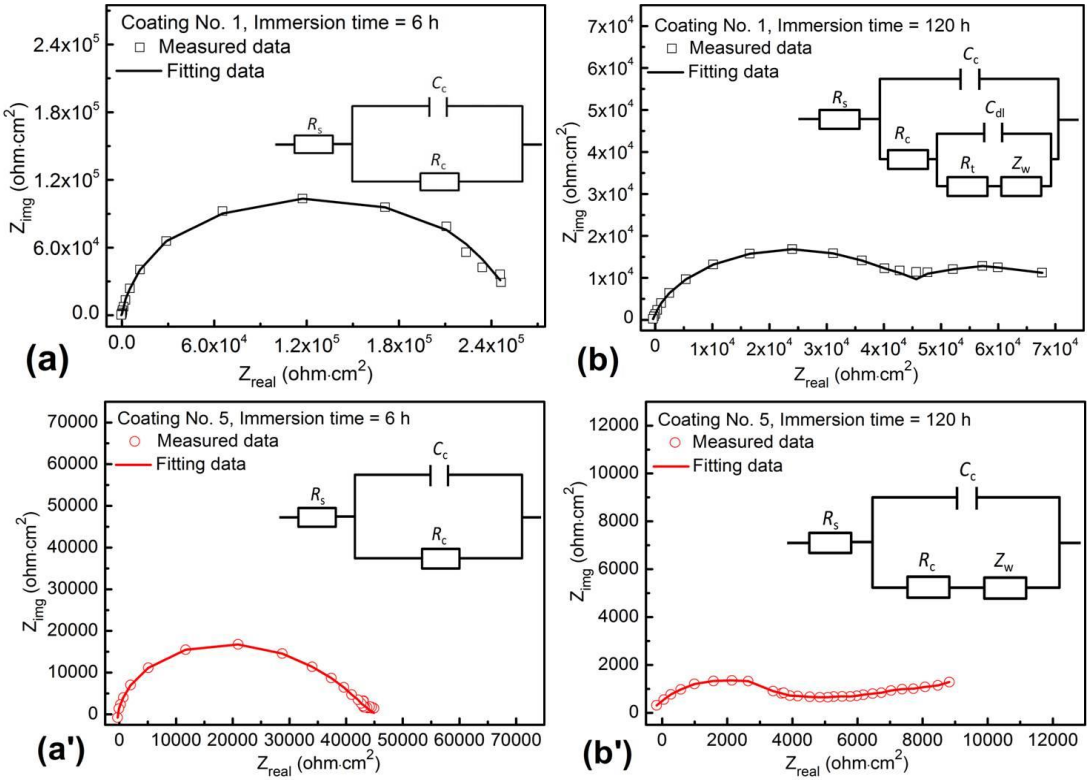

Figure 6. Nyquist diagrams for Coating No. 1 (a) and (b), and Coating No. 5 (a') and (b') in 3.5 wt.% NaCl solution as a function of immersion time

For Nyquist diagrams in Fig. 6(a) and Fig. 6(a'), only one single capacitive loop has been observed during the whole frequency ranges, indicating that only one time constant exists and NaCl solution has not penetrated to the coating/substrate interface at immersion time of 6 h [37]. Under this condition, the corresponding equivalent circuit for EIS data fitting given at the upper-right corner of Fig. 6(a) and Fig. 6(a') can also be expressed by Eq. (1). However, it has been found that after a longer period of 120 h immersion, the presence of rust spots and macro-pores can be clearly observed on the two coatings surface. With the formation of macro-pores on coating surface, the reactants can easily get through the coating to the coating/substrate interface, and the existed reactants concentration gradient in the waterborne coating disappears [48]. Meanwhile, a new reactants concentration gradient at the coating/substrate interface forms due to the fast consumption in reactants paralleled by the substrate corrosion, and the diffusion process exists at the coating/substrate interface area close to the substrate [49]. Usually, the period after the appearance of rust spots on coating surface was regarded as the late immersion stage [50]. In this condition, there are two cases in illustrating the EIS spectra, depending on the surface porosity of waterborne coating and its detachment area from the underlying substrate. With a lower surface porosity and smaller detachment area in the waterborne coating, the coating can still have the barrier and protection effect to the underlying substrate. Under this condition, Nyquist diagram usually has the feature as shown in Fig. 6(b), and the corresponding equivalent circuit for EIS data fitting given at the upper-right corner of Fig. 6(b) can be expressed by Eq. (4):

$$Z = R_s + \frac{1}{j\omega C_c + \frac{1}{R_c + \frac{1}{j\omega C_{dl} + \frac{1}{R_t + Z_w}}}} \quad (4)$$

where R_s is solution resistance; C_c is coating capacitance; R_c is coating resistance; C_{dl} is double layer capacitance; R_t is substrate dissolution resistance, and Z_w is diffusion impedance.

With a much higher surface porosity and lager detachment area of the coating, it has lost its barrier and protection effect to the steel substrate. At this time, Nyquist diagram usually has the feature as shown in Fig. 6(b'), and the corresponding coating impedance can be expressed by Eq. (5):

$$Z = R_s + \frac{1}{j\omega C_c + \frac{1}{R_c + Z_w}} \quad (5)$$

where R_s is solution resistance; C_c is coating capacitance; R_c is coating resistance, and Z_w is diffusion impedance.

The fitted C_c and R_c of Coating No. 1 and Coating No. 5 after 6 h and 120 h immersion are shown in Figure 7. The standard deviations x^2 were in the order of 10^{-5}, and the relative error for each parameter was less than 10 %. Clearly, as the immersion time proceeds, C_c increases and R_c decrease of both Coating No. 1 and Coating No. 5. Fig. 7(a) shows that Coating No. 1 with pigments addition has a higher R_c than Coating No. 5 without pigments addition at 6 h immersion, indicating the better corrosion resistance by pigments addition. At 120 h immersion, although R_c of the two coatings decreases obviously, the decreasing rate of Coating No. 5 is higher than that of Coating No. 1, indicating a much more serious corrosion damage for Coating No. 5 during the immersion period from 6 h to 120 h. For C_c evolution in Fig. 7(b), it has an inverse proportion relationship with R_c in Fig. 7(a). In addition, C_c for Coating No. 1 increases a little, but it increases greatly for Coating No. 5, also indicating the more serious corrosion damage for Coating No. 5. Moreover, the obviously increased C_c for Coating No. 5 also indicates its serious corrosion attack by NaCl solution and the substantial protective effect of pigments addition to the waterborne coating.

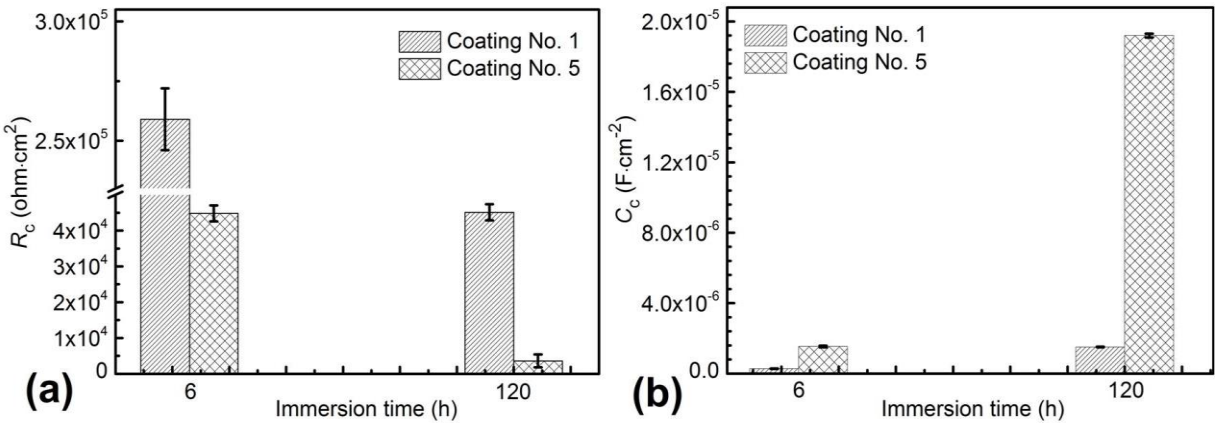

Figure 7. Fitted R_c (a) and C_c (b) evolution of Coating No. 1 and Coating No. 5 at immersion time of 6 h and 120 h

3.5 Effect of immersion time on corrosion behavior waterborne coating

To investigate the corrosion behavior of waterborne epoxy ester coating as a function of immersion time in 3.5 wt.% NaCl solution, Coating No. 1 has been immersed for different hours at room temperature for EIS measurements. Figure 8 shows Nyquist diagrams evolution of Coating No. 1 as a function of immersion time. Fig. 8(a) shows that the waterborne coating has a single capacitive loop with a large diameter, indicating the better shielding effect of the waterborne coating and the little amount of NaCl solution penetration into the coating at the initial immersion stage [51]. As the immersion time proceeds to 72 h, Fig. 8(b) shows that the waterborne coating still has a single capacitive loop but with a greatly decreased diameter, indicating that the coating at this time still has corrosion protection effect to the steel substrate and NaCl electrolyte has penetrated into the waterborne coating but has not reach the coating/substrate interface [52]. However, as the immersion time proceeds to 120 h, Fig. 8(c) shows that two time constants have been observed in Nyquist diagram, indicating that NaCl electrolyte has reached the coating/steel interface, and the steel corrosion has occurred but the coating still has wet adhesion to the substrate [53]. Moreover, when the immersion time further proceeds to 240, Fig. 8(d) shows that the diameter of capacitive loop at high frequency range further decreases compared with the result in Fig. 8(c), indicating the much more serious corrosion attack on the underlying steel substrate [54].

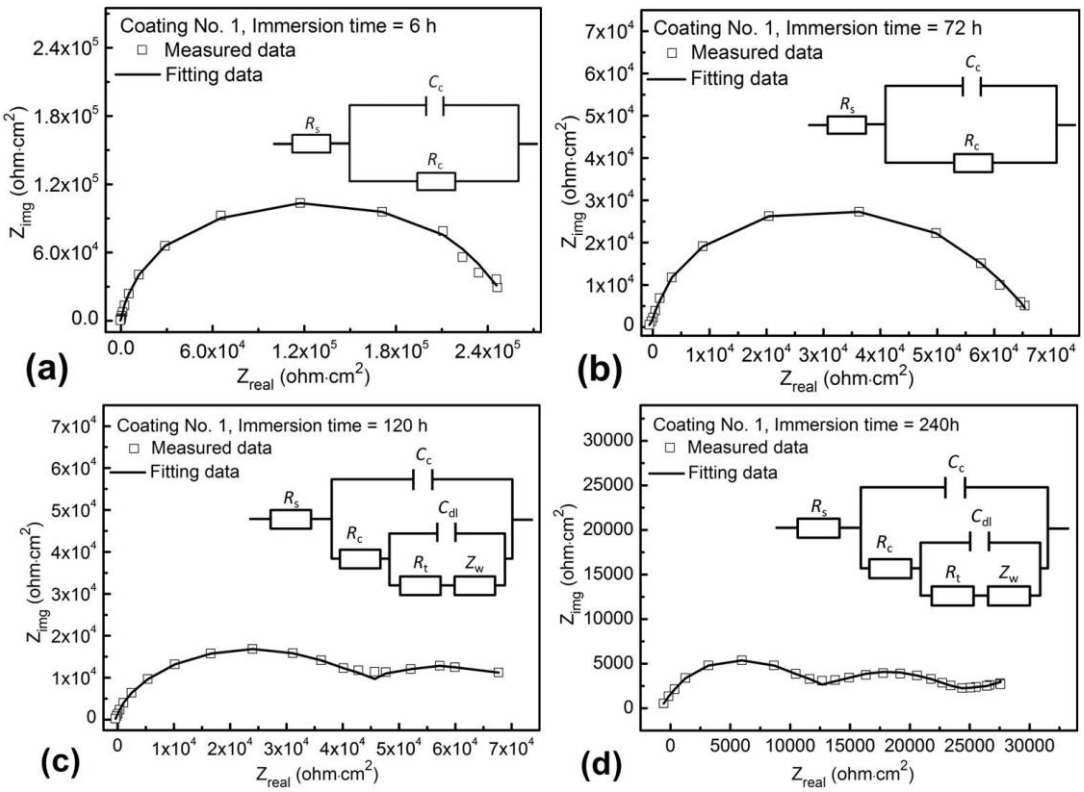

Figure 8. Nyquist diagrams for Coating No. 1 after immersion in 3.5 wt.% NaCl solution as a function of immersion time. (a) 6 h; (b) 72 h; (c) 120 h; (d) 240 h

Equivalent circuits have also been used to fit the EIS data to further understand the effect of immersion time on corrosion behavior of waterborne coating in 3.5 wt.% NaCl solution. For Nyquist diagrams in Fig. 8(a), Fig. 8(b), Fig. 8(c) and Fig. 8(d), the used equivalent circuit of each has been given at the upper-right corner in the corresponding figure, and the details of the equivalent circuits have been discussed in the above sections. The standard deviations x^2 were in the order of 10^{-5}, and the relative error for each parameter was less than 10 %. Figure 9 shows the fitted coating resistance R_c and capacitance C_c as a function of immersion time. Clearly, R_c has an inverse proportion relationship with C_c, and R_c decreases and C_c increases as the immersion time proceeds. At 6 h immersion time, the waterborne coating has much higher R_c and lower C_c, indicating the ideal shielding effect and corrosion protection effect of the coating to steel substrate. However, as the immersion time proceeds to 240 h, R_c greatly decreases, indicating its gradual lost in shielding effect and corrosion protection effect to the steel substrate [55-56]. The variation of R_c and C_c matches well with EIS results in Fig. 8.

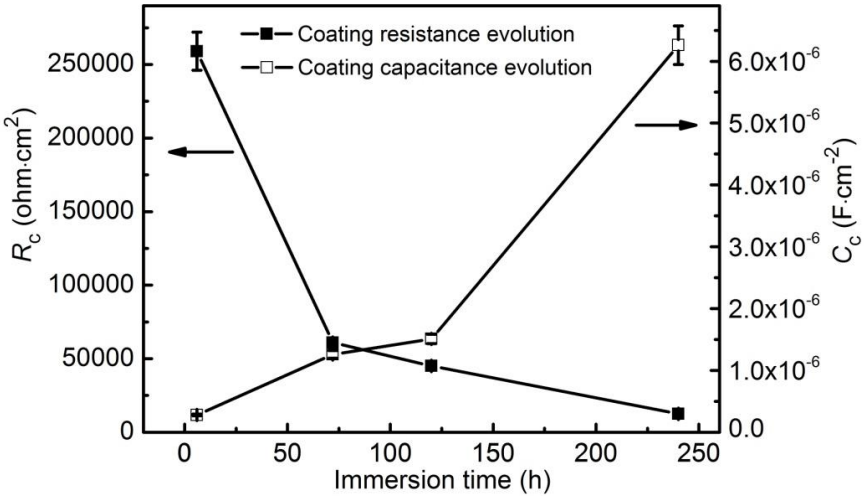

Figure 9. Fitted coating resistance R_c and coating capacitance C_c evolution of Coating No. 1 as a function of immersion time

Therefore, for the corrosion of waterborne coating in 3.5 wt.% NaCl solution, the corrosion time is also a critical factor in determining its corrosion protection effect, and in practice avoiding the electrolyte accumulation on the coating surface for a long time and keeping it dry is necessary for maintaining the protection effect of waterborne coating.

4. CONCLUSIONS

(1) As the same to other organic coating, shielding effect to corrosion electrolyte is also the main protective effect of waterborne organic coating in NaCl solution. Higher water resistance and crosslinking degree contribute to higher corrosion resistance of the waterborne coating. However, enhanced crosslinking degree may lead to decreased water resistance of the waterborne coating, and it is necessary to minimize the content of hydrophilic groups in the waterborne coating while ensuring the qualified crosslinking degree for improving corrosion resistance of waterborne coating.

(2) Pigments of $ZnMoO_4$ and $Zn_3(PO_4)_2$ addition to the waterborne epoxy ester coating can greatly improve the corrosion resistance of the coating, and waterborne epoxy ester varnish coating without pigments addition degrades quickly in NaCl solution as the immersion time proceeds.

(3) For the corrosion evolution of waterborne epoxy ester coating in NaCl solution, the coating has better shielding effect at 6 h immersion. At 72 h immersion, the coating still has corrosion protection effect to the steel substrate and NaCl electrolyte has penetrated into the waterborne coating but has not reach the coating/substrate interface. At 120 h immersion time, NaCl electrolyte has reached the coating/steel interface, and the steel corrosion has occurred. At 240 h immersion time, serious corrosion attack occurs on the steel substrate, and the waterborne coating lost its shielding effect and corrosion protection effect to the underlying steel substrate.

ACKNOWLEDGEMENTS
This work was supported by the Supporting Plan for Excellent Talents in Institutions of Higher Education of Liaoning Province (No. LR2015044), and the authors acknowledge the assistance.

References

1. V. D. Athawale and R. V. Nimbalkar, *J. Am. Oil Chem. Soc*., 88 (2011) 159.
2. G. Bierwagin, D. Tallman, J. P. Li, L. Y. He and C. Jeffeoate, *Prog. Org. Coat.*, 41 (2003) 148.
3. M. C. Deya, G. Blustein, R. Romagnoli and B. D. Amo, *Surf. Coat. Technol*., 150 (2002) 133.
4. X. Wang, S. Chen and R. Ding, *Int. J. Electrochem. Sci.*, 14 (2019) 3553.
5. J. Yoon and P. A. Lovell, *Macromol. Chem. Phys*., 209 (2008) 279.
6. S. O. Han and L. T. Drzal, *Eur. Polym. J*., 39 (2003) 1791.
7. M. J. Yang and J. D. Zhang, *J. Mater. Sci.*, 40 (2005) 4403.
8. W. Sephentait, *J. Coat. Teehnol*., 75 (2003) 45.
9. U. Kanai and T. Amari, *Prog. Org. Coat.*, 45 (2002) 267.
10. Y. Su, S. H. Qiu and Yu Liu, *Int. J. Electrochem. Sci.*, 14 (2019) 4595.
11. O. D. Cabaret, B. M. Vaca, D. Bourissou, *Chem. Rev*., 104 (2004) 6147.
12. P. A. Sorensen, S. Kiil, K. D. Johansen and C. E. Weinell, *J. Coat. Technol. Res.*, 6 (2009) 135.
13. S. W. Zhang, R. Liu, J. Q. Jiang and H. Y. Bai, *Prog. Org. Coat*., 65 (2009) 56.
14. Z. J. Pan, *Mater. Prot*., 22 (1994) 9.
15. D. Zhang, H. Q. Zhang and S. Zhao, *Int. J. Electrochem. Sci*., 14 (2019) 4659.
16. M. L. Yang, J. H. Wu, D. Q. Fang, B. Li and Y. Yang, *J. Mater. Sci. Technol*., 34 (2018) 2464.
17. J. Jang and E. K. Kim, *J. Appl. Polym. Sci*., 71 (1999) 585.
18. J. D. Zhang, M. J. Yang, Y. R. Zhu and H. Yang, *Polym. Int*., 55 (2006) 951.
19. C. Vilela, A. F. Sousa, A. C. Fonseca, A. C. Serra and A. J. D. Silvestre, *Polym. Chem*., 5 (2014) 3119.
20. C. Perez, A. Collazo, M. Izquierdo, P. Merino and X. R. Novoa, *Prog. Org. Coat*., 37 (1999) 169.
21. T. Westing, *Prog. Org. Coat.*, 23 (1993) 89.
22. P. A. Sorensen, S. Kiil, K. Dam-Johansen and C. E. Weinell, *J. Coat. Technol. Res*., 6 (2009) 135.
23. T. Xu, H. Q Li, J. Song and G. L. Wang, *Int. J. Electrochem. Sci*., 14 (2019) 5051.
24. A. Wegmann, *Prog. Org. Coat*., 32 (1997) 231.
25. M. Khan, A. A. Khurram, T. H. Li, T. K. Zhao and V. Patel, *J. Mater. Sci. Technol*., 34 (2018) 2424.
26. G. Tillet, B. Boutevin and B. Ameduri, *Prog. Polym. Sci*., 36 (2011) 191.
27. L. S. Tang, M. Zhang, S. F. Zhang, J. Z. Yang, *Prog. Org. Coat.*, 49 (2004) 54.

28. Z. Y. Fan, Q. Xu, Y. Xu and N. Lin, *Int. J. Electrochem. Sci*., 14 (2019) 7487.
29. V. Baukh, H. P. Huinink, O. C. Adan, S. J. Erich and L. G. Vanderven, *Macromolecules,* 44 (2011) 4863.
30. F. Mazuel, C. Bui, B. Charleux, E. C. Deliry and M. A. Winnik, *Macromolecules,* 37 (2004) 6141.
31. G. L. Gyorik, T. Pajkossy and B. Lengyel, *Prog. Org. Coat*., 59 (2007) 95.
32. S. W. Strunz, *Prog. Org. Coat*., 39 (2000) 49.
33. T. Kolås, A. Røyset, M. Grandcolas and A. Lacau, *Solar Energy Mater. Solar Cells*, 196 (2019) 94.
34. N. Siyab, S. Tenbusch, S. Willis, C. Lowe and J. Maxted, *J. Coat. Technol. Res*., 13 (2016) 629.
35. S. Cotugno, D. Larobina, G. Mensitieri, P. Musto and G. Ragosta, *Polymer*, 42 (2001) 6431.
36. S. X. Deng, J. Y. Wu, Y. D Li, G. Wang and F. C. Liu, *Int. J. Electrochem. Sci*., 14 (2019) 315.
37. A. Blencowe, J. F. Tan, T. K. Goh, G. G. Qiao, *Polymer*, 50 (2009) 5.
38. P. A. Tamirisa and D. W. Hess, *Macromolecules*, 39 (2006) 7092.
39. S. Gach, S. Olschok and U. Reisgen, Materialwiss. *Werkstofftech*., 50 (2019**)** 365.
40. R. E. Drumright, P. R. Gruber, D. E. Henton, *Adv. Mater*., 12 (2000) 1841.
41. G. Pan, L. Wu, Z. Zhang and D. Li, *J. Appl. Polym. Sci*., 83 (2002) 1736.
42. D. Yin, Z. X. Yu and L. G. Chen, *Int. J. Electrochem. Sci*., 14 (2019) 4240.
43. S. Y. Liu, A. Q. Wang, S. J. Lu and J. P. Xie, Materialwiss. *Werkstofftech.*, 49 (2018) 49 1213.
44. B. V. Jegdic, J. B. Bajat, J. P. Popic , S. I. Stevanovic and V. B. Stankovic, *Corros. Sci.*, 53 (2011) 2872.
45. A. Caretto, V. Passoni, N. Brenna, M. Sitta, and G. Griffini, *ACS Sustainable Chem. Eng*., 6 (2018**)** 14125.
46. E. Gubbels, L. J. Walc, B. A. Noordover and C. Koning, *Eur. Polym. J.*, 49 (2013) 3188.
47. H. H. Pham and M. A. Winnik, *Macromolecules*, 39 (2006) 1425.
48. Z. W. Wicks, N. Frank, S. P. Pappas and D. A. Wicks, Polyester Resins. In Organic Coatings: Science and Technology, 3rd ed., John Wiley & Sons, Inc., (2007) Hoboken, NJ.
49. C. N. Cao, Principles of Electrochemistry of Corrosion, Chemical Industry Press, (2004) Beijing, China.
50. D. R. Miller and C. W. Macosko, *J. Polym. Sci., B: Polym. Phys*., 26 (1988) 1.
51. D. R. Bauer and G. F. Budde, *Ind. Eng. Chem. Prod. Res. Dev*., 20 (1981) 674.
52. G.K. Wanderwel and O. C. G. Adan, *Prog. Org. Coat*., 37 (1999) 1.
53. R. G. Joshi, T. Provder, P. Ziemer, W. J. Mao and F. N. Jones, *J. Coat. Technol. Res*., 6 (2009) 47.
54. W. G. Ji, J. M. Hu, J. Q. Zhang and C.N. Cao, *Corros. Sci.*, 48 (2006) 3731.
55. L. K. Wu, J. T. Zhang, J. M. Hu and J. Q. Zhang, *Corros. Sci*., 56 (2012) 58.
56. J. T. Zhang, J. M. Hu, J. Q. Zhang and C. N. Cao, *Prog. Org. Coat*., 51 (2004) 145.